Available online at www.sciencedirect.com
ScienceDirect
Journal of Sound and Vibration 299 (2007) 1074–1093
JOURNAL OF SOUND AND VIBRATION
www.elsevier.com/locate/jsvi

Free vibrations of the partial-interaction composite members with axial force

Yu-Fei Wu[a,*], Rongqiao Xu[b], Weiqiu Chen[b]

[a]*Department of Building and Construction, City University of Hong Kong, Tat Chee Avenue, Kowloon, Hong Kong*
[b]*Department of Civil Engineering, Zhejiang University, Hangzhou 310027, PR China*

Received 30 June 2006; received in revised form 7 August 2006; accepted 11 August 2006
Available online 4 October 2006

Abstract

The governing differential equations of motion are derived for the partial-interaction composite members with axial force and the solutions of free vibrations are presented under common boundary conditions. An exact analytical solution for a simply supported case is obtained. If the slip at the interface of the composite member is ignored, both the equations and the solution can be degenerated to those corresponding to the elementary beam theory as they should be. An approximate simple expression is also proposed to predict the fundamental frequency of the partial-interaction composite members with axial force, which is of practical interest. Finally, numerical results and the effects of the axial force, shear connector rigidity and other parameters upon the frequencies are presented and discussed in detail.

1. Introduction

Composite members have a wide application in engineering structures since they are stronger, stiffer and more ductile than the sum of the individual elements. The steel-concrete composite beams are the most familiar where concrete slab is used in compressive portion of the member and steel beam in the tensile portion. Composite members are also applicable to retrofitting of existing structures in practice [1]. The shear connection is usually provided by the headed stud shear connectors at the interface between the two materials. Because of the flexibility of the shear connectors, longitudinal slip at the interface will occur and make the behavior of composite structures complex. This phenomenon is well known as the partial interaction. Newmark et al. [2] developed a classical linear elastic partial-interaction theory for composite beams based on the elementary beam theory. Goodman [3] independently presented the theories for layered wood systems with interlayer slip. Girhammar and Gopu [4] presented analysis of composite beam columns with partial interaction subjected to transverse and axial loading. Using this theory, Wang [5] proposed a simplified method for designers to predict the maximum deflection of a composite beam with partial interaction at working load based on the stiffness of its shear connectors. Wu et al. [6] investigated a cantilever column subjected to lateral and axial forces and presented the non-linear slip distributions. They also discussed key

*Corresponding author. Tel.: +852 27844259; fax: +852 27887612.
E-mail address: yfwu00@cityu.edu.hk (Y.-F. Wu).

0022-460X/$ - see front matter © 2006 Published by Elsevier Ltd.
doi:10.1016/j.jsv.2006.08.008

parameters that govern the longitudinal slip and affect the deflection in detail. Fabbrocino et al. [7] and Seracino et al. [8] extended these theories to continuous beams and emphasized the effect of the negative bending moment. Besides these analytical works, some numerical methods were also introduced to investigate the mechanical behaviors of partial-interaction composite beams [9–12], which mainly concerned the finite element method.

However, investigations concerning the dynamic responses of composite beams or columns with partial interaction are scarce. Introducing the inertia force by d'Alembert's principle, Girhammar and Pan [13] extended their theory for static equilibrium of partial-interaction composite beams to dynamic problems and presented the governing differential equation of motion, which excluded the effect of the axial force. Its improved theory that took the viscous damping into account was then presented by Adam and Jeschko [14].

This paper presents a theory for the dynamic analysis of partial-interaction composite members with axial forces, which is applicable to, for example, plated reinforced concrete columns [1] and prestressed composite beams. Both the governing equations and their solutions can be degenerated to that of the generic beam theory as they should be when the slip at the interface of the composite beams is zero. Approximate expressions based on the exact solution for a simply supported case are also proposed to predict the fundamental frequency, which is of practical interest, of the partial-interaction composite members with axial force. The effects of the axial force, shear connector rigidity and other parameters upon the frequencies are discussed in detail through the solutions and their numerical results in the end.

2. Governing equation

2.1. Problems and assumptions

Let us now consider the transverse vibrations of a composite member with two sub-elements of different materials in the $x-y$ plane as shown in Fig. 1a. The x-axis is the neutral axis of the full-interaction composite beam. E_i, I_i, A_i and m_i ($i = 1, 2$) denote the Young's modulus, area moment of inertia, cross-sectional area and the mass of the two sub-elements per unit length, respectively. L is the length of the beam and H signifies the axial force, which is constant and positive for tension while negative for compression. It is assumed, for convenience, that the axial force H is acted at the centroid of the full interaction cross-section. In fact, if the axial load has an eccentric distance e from the centroid, only an additional bend moment He has to be superimposed. The symbols h, h_1, h_2 and y_2, standing for a few distances, are plotted in Fig. 1b.

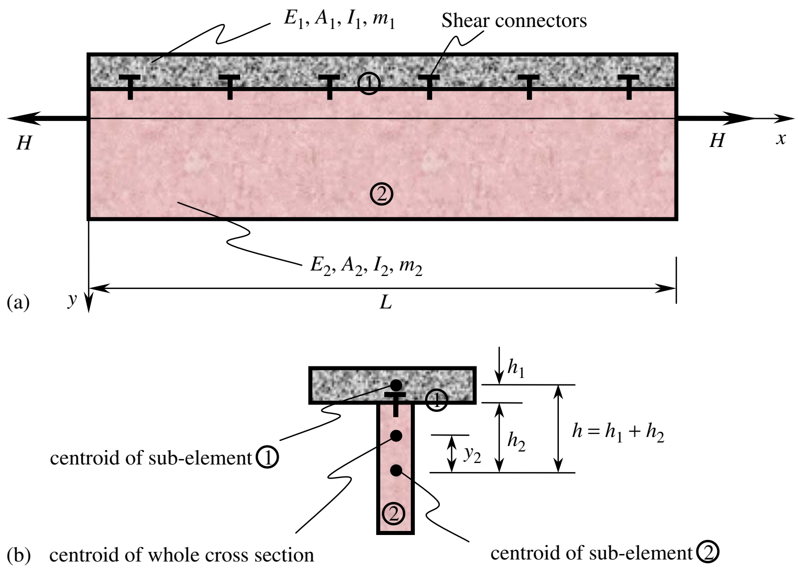

Fig. 1. Composite member with axial force and the coordinate system.

Although the assumptions used in the one-dimensional theory of linear elastic partial-interaction composite members have been described in Refs. [4,6,13], they are repeated herein for the integrity of the deduction: (1) All the constitutive materials behave linearly and the deformations are small; (2) Bernoulli's hypothesis of plane cross-section applies to individual sub-elements; (3) the shear connectors between the two sub-elements are continuous and uniformly distributed longitudinally; and (4) no transverse separation occurs on the contact interface, therefore the curvature is the same for both the sub-elements at the same point.

2.2. Equilibrium of forces

Fig. 2 shows a free-body diagram of an infinitesimal element of length dx with internal, inertial and external distributed actions upon it. Bending moment, shear force and normal force are denoted by M, Q and N, respectively. A comma before subscript x or t indicates the partial differential with respect to coordinate x or time t, respectively.

According to the hypothesis of small deformation and the dynamic equilibriums of the force and bending moment, we have

$$N = H, \tag{1}$$

$$Q_{,x} = -q + mv_{,tt} - Nv_{,xx}, \tag{2}$$

$$M_{,x} = Q, \tag{3}$$

where H is a constant. The dashed arrows labeled by N_1, N_2, M_1 and M_2 in Fig. 2 are the axial force and bending moment of each sub-element, respectively. They are statically equivalent ones of the axial force N and bending moment M of the whole cross-section, namely

$$H = N = N_1 + N_2, \tag{4}$$

$$M = M_1 + M_2 - N_1 h + Hy_2, \tag{5}$$

where $h = h_1 + h_2$ is the distance between the two centroids of sub-elements 1 and 2, y_2 denotes the distance of the centroid of the whole section to the centroid of sub-element 2, namely,

$$y_2 = \frac{E_1A_1}{E_1A_1 + E_2A_2}h = \frac{E_1A_1}{\Sigma EA}h, \tag{6}$$

where $\Sigma EA = E_1A_1 + E_2A_2$ is the axial rigidity of the full composite members.

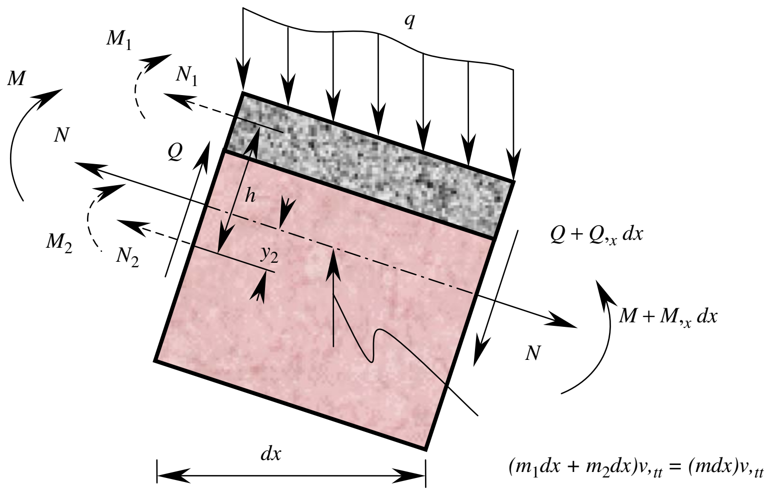

Fig. 2. Deformed infinitesimal element.

Taking into account the interlayer slip, Fig. 3 exhibits the forces in the axial direction of each sub-element, including the interlayer shear force provided by the shear connectors and two axial forces N_1 and N_2. The equilibrium conditions of forces of sub-elements 1 and 2 in the axial direction give

$$N_{1,x} = -N_{2,x} = -Q_s. \tag{7}$$

2.3. Kinematics of the slip of the interface

Due to the Bernoulli's hypothesis of plane cross-section and the assumption of no transverse separation on the interface, the geometrical relation between the slip u_s with the deflection v and the longitudinal displacement u is given by (see Fig. 4)

$$u_s = u_2 - u_1 + v_{,x}h, \tag{8}$$

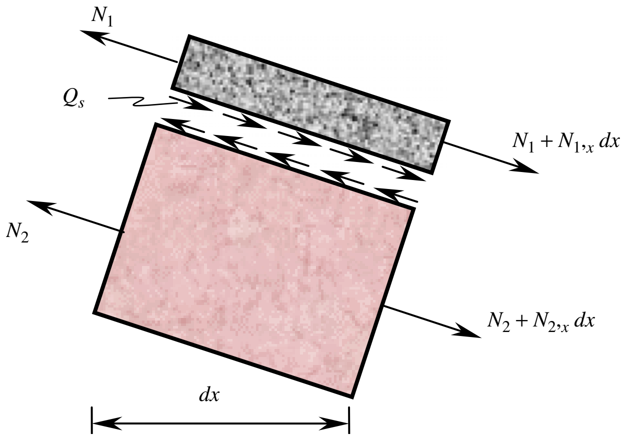

Fig. 3. Forces in axial direction (longitudinal direction).

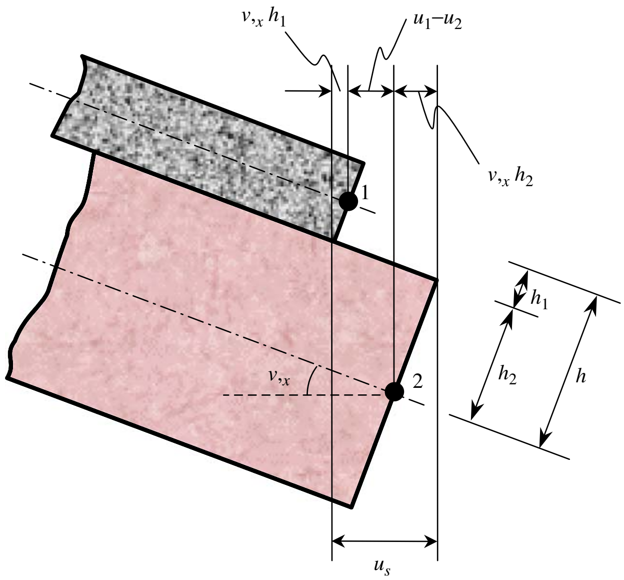

Fig. 4. Geometrical relationship between u_s and v and u.

where u_1 and u_2 are the longitudinal displacement at the centroids of sub-elements 1 and 2, respectively. Differentiating Eq. (8) with respect to x results in

$$u_{s,x} = \varepsilon_2 - \varepsilon_1 + v_{,xx}h, \tag{9}$$

where ε_1 and ε_2 are the longitudinal strains at the centroids of sub-elements 1 and 2, respectively.

2.4. The relations of the deformation and the resultants

Since the assumption of plane section is applicable to each sub-element, the well-known relation of curvature and bending moment satisfies

$$v_{,xx} = -\frac{M_1}{E_1 I_1} = -\frac{M_2}{E_2 I_2} \tag{10}$$

And the shear connectors between the two sub-elements are assumed to be continuous and uniformly distributed longitudinally, we have

$$Q_s = k_s u_s, \tag{11}$$

where k_s denotes the shear stiffness of the shear connector per unit length. Another relation of the longitudinal strain and the axial force is readily obtained as

$$\varepsilon_1 = \frac{N_1}{E_1 A_1}, \quad \varepsilon_2 = \frac{N_2}{E_2 A_2}. \tag{12}$$

2.5. Governing equation

Substitution Eq. (10) into Eq. (5) yields

$$v_{,xx} = -\frac{M + N_1 h - H y_2}{\Sigma EI}, \tag{13}$$

where $\Sigma EI = E_1 I_1 + E_2 I_2$ is the area moment of inertia of no-interaction composite members. Eliminating the bending moment M from Eqs. (1)–(3) and (13) gives

$$v_{,xxxx} = \frac{q + H v_{,xx} - m v_{,tt} - N_{1,xx} h}{\Sigma EI} \tag{14}$$

Substituting Eq. (12) into Eq. (9) produces

$$u_{s,x} = \frac{N_2}{E_2 A_2} - \frac{N_1}{E_1 A_1} + v_{,xx} h. \tag{15}$$

We then can express the derivative of the interlayer shear force $Q_{s,x}$ in terms of N_1 and $v_{,xx}$ from Eqs. (4), (11) and (15), as follows:

$$Q_{s,x} = k_s \left(\frac{H - N_1}{E_2 A_2} - \frac{N_1}{E_1 A_1} + v_{,xx} h \right). \tag{16}$$

Using the relation of Q_s and N_1 given by Eq. (7), we obtain another relation of N_1 and v

$$N_{1,xx} = -k_s \left(\frac{H - N_1}{E_2 A_2} - \frac{N_1}{E_1 A_1} + v_{,xx} h \right). \tag{17}$$

To obtain the differential equation of N_1, eliminating the deflection v from Eqs. (13) and (17) and rearrangement of terms yield

$$N_{1,xx} - \alpha^2 N_1 = \frac{k_s h}{\Sigma EI} M - k_s \left(\frac{1}{E_2 A_2} + \frac{y_2 h}{\Sigma EI} \right) H, \tag{18}$$

where α^2 is a parameter involving the stiffness of the shear connectors and given by

$$\alpha^2 = k_s\left(\frac{1}{E_1A_1} + \frac{1}{E_2A_2} + \frac{h^2}{\Sigma EI}\right). \tag{19}$$

Eliminating the bending moment M using Eqs. (3) and (18) produces

$$N_{1,xxxx} - \alpha^2 N_{1,xx} = -\frac{k_s h}{\Sigma EI}(q + Hv_{,xx} - mv_{,tt}). \tag{20}$$

Eqs. (14) and (20) are a coupled differential equation set of the deflection v and axial force N_1. For convenience, they can be reduced to one governing differential equation in terms of the unique variable v, namely

$$\overline{EI}v_{,xxxxxx} - (\overline{EI}\alpha^2 + \beta^2 H)v_{,xxxx} + \beta^2 mv_{,xxtt} + \alpha^2 Hv_{,xx} - \alpha^2 mv_{,tt} = -\alpha^2 q + \beta^2 q_{,xx}, \tag{21}$$

where $\overline{EI}$ is the flexural stiffness of the composite member when the stiffness of the shear connector approaches infinity, i.e., of the full-interaction composite members, and β^2 is another important parameter indicating the cross-sectional property of the composite members; and they are defined as

$$\overline{EI} = \Sigma EI + \frac{E_1A_1\,E_2A_2}{E_1A_1 + E_2A_2}h^2, \quad \beta^2 = \frac{\overline{EI}}{\Sigma EI}. \tag{22}$$

It should be noticed that Eq. (21) can be degenerated to two limit cases, i.e., full interaction and non-composite action. For instance, if the shear connector is rigid, namely, k_s approaches infinite and $\alpha_1^2 \to \infty$, Eq. (21) can be degenerated to

$$\overline{EI}v_{,xxxx} - Hv_{,xx} + mv_{,tt} = q, \tag{23}$$

which is a governing differential equation of a full-interaction composite beams with axial force H. For another limit case, namely, k_s approaches zero ($\alpha^2 = 0$), Eq. (21) becomes

$$\Sigma EIv_{,xxxx} - Hv_{,xx} + mv_{,tt} = q. \tag{24}$$

Once the transverse load q is known, the deflection v of the member can be solved from Eq. (21) for specific boundary and initial conditions. Then the internal forces can be determined in terms of v as follows:

$$M = \overline{EI}\left[\frac{1}{\alpha^2}v_{,xxxx} - \left(1 + \frac{H}{\alpha^2\Sigma EI}\right)v_{,xx} + \frac{mv_{,tt} - q}{\alpha^2\Sigma EI}\right], \quad Q = M_{,x}, \tag{25}$$

$$M_1 = -E_1I_1v_{,xx}, \quad M_2 = -E_2I_2v_{,xx}, \tag{26}$$

$$N_1 = \frac{\overline{EI}}{h\alpha^2}\left[-v_{,xxxx} + \left(\alpha^2 + \frac{H}{\Sigma EI} - \frac{\alpha^2}{\beta^2}\right)v_{,xx} - \frac{mv_{,tt} - q}{\Sigma EI} + \frac{\alpha^2 Hy_2}{\overline{EI}}\right], \quad N_2 = H - N_1, \tag{27}$$

$$Q_s = \frac{1}{h}(M_{,x} + \Sigma EIv_{,xxx}). \tag{28}$$

2.6. Boundary conditions

For the governing differential equation (21) of six-order, a total of six boundary conditions are necessary to determine the integral constants. In practice, three classic boundary conditions at the ends of a member are usually considered, which are (S) simply supported, (C) clamped and (F) free. For the simply supported end, the boundary conditions $M_1 = M_2 = 0$, $v = 0$ and $N_1 = Hy_2/h$ yield, according to Eqs. (26) and (27):

$$v = 0, \quad v_{,xx} = 0, \quad \Sigma EIv_{,xxxx} - q = 0. \tag{29}$$

When the end is clamped, it can be concluded that $v = 0$, $v_{,x} = 0$ and $u_s = 0$. The last one of these conditions implies that $N_{1,x} = -Q_s = 0$ in accordance with Eqs. (7) and (11). Then the boundary conditions at a clamped end can be rendered in terms of v as

$$v = 0, \quad v_{,xx} = 0, \quad v_{,xxxxx} - \alpha^2\left(1 - \frac{1}{\beta^2} + \frac{H}{\alpha^2\Sigma EI}\right)v_{,xxx} - \frac{q_{,x}}{\Sigma EI} = 0. \tag{30}$$

The third conditions corresponding to the free end are $M_1 = M_2 = 0$, $Q + Hv_{,x} = 0$ and $N_1 = Hy_2/h$. By employing Eqs. (25)–(27), the following equations are obtained:

$$\begin{aligned} &v_{,xx} = 0, \quad v_{,xxxx} + \frac{m}{\Sigma EI}v_{,tt} - \frac{q_{,x}}{\Sigma EI} = 0, \\ &v_{,xxxxx} - \left(\alpha^2 + \frac{H}{\Sigma EI}\right)v_{,xxx} + \frac{mv_{,xtt} - q_{,x}}{\Sigma EI} + \frac{\alpha^2 H}{\overline{EI}}v_{,x} = 0. \end{aligned} \tag{31}$$

Since a member with finite length has two ends and three end conditions, i.e., (S) simply supported, (C) clamped and (F) free, exist at each end, six possible cases can be obtained through a combination of them. They are denoted by SS, SC, SF, CC, CF and FF, in which SS means both two ends are simply supported, and so on. However, four cases SS, SC, CC and CF are applicable in practice and are considered in the rest of this paper.

3. Solutions of free vibrations

If the member vibrates freely with a resonant frequency ω_n, we can assume

$$v(x,t) = v_0\tilde{v}(\xi)\exp(\mathrm{j}\omega_n t), \tag{32}$$

where v_0 is a length parameter giving the amplitude of the deflection, j denotes the imaginary unit and $\xi = x/L$ signifies the non-dimensional coordinate in the x direction. Substitution of Eq. (32) into the governing differential equation (21) and eliminating the right-hand side yield

$$\tilde{v}_{,\xi\xi\xi\xi\xi\xi} - (\tilde{\alpha}^2 + \beta^2\tilde{H})\tilde{v}_{,\xi\xi\xi\xi} - (\beta^2\tilde{\omega}_n^2 - \tilde{\alpha}^2\tilde{H})\tilde{v}_{,\xi\xi} + \tilde{\alpha}^2\tilde{\omega}_n^2\tilde{v} = 0, \tag{33}$$

where $\tilde{\alpha}$, $\tilde{H}$ and $\tilde{\omega}_n$ are non-dimensional quantities corresponding to α, H and ω_n as

$$\tilde{\alpha}^2 = \alpha^2 L^2, \quad \tilde{H} = \frac{HL^2}{\overline{EI}}, \quad \tilde{\omega}_n^2 = \frac{m\omega_n^2 L^4}{\overline{EI}}. \tag{34}$$

The general solutions of the homogeneous differential equation (33) are based on the root characteristic of its eigen equation

$$\lambda^6 - (\tilde{\alpha}^2 + \beta^2\tilde{H})\lambda^4 - (\beta^2\tilde{\omega}_n^2 - \tilde{\alpha}^2\tilde{H})\lambda^2 + \tilde{\alpha}^2\tilde{\omega}_n^2 = 0. \tag{35}$$

Introducing a symbol $\Lambda = \lambda^2$, Eq. (35) becomes

$$\Lambda^3 - (\tilde{\alpha}^2 + \beta^2\tilde{H})\Lambda^2 - (\beta^2\tilde{\omega}_n^2 - \tilde{\alpha}^2\tilde{H})\Lambda + \tilde{\alpha}^2\tilde{\omega}_n^2 = 0. \tag{36}$$

It is a cubic equation of one variable. It can be shown that all three roots of Eq. (36) are real and one is negative while the other two are positive (see Appendix A in detail). Letting $\Lambda_1 < 0$ and $\Lambda_2 > 0$ and $\Lambda_3 > 0$ denote the three roots of Eq. (36), the six roots of Eq. (35) are then $\pm\lambda_1$j, $\pm\lambda_2$ and $\pm\lambda_3$, with

$$\lambda_1 = \sqrt{-\Lambda_1}, \quad \lambda_2 = \sqrt{\Lambda_2}, \quad \lambda_3 = \sqrt{\Lambda_3}. \tag{37}$$

Consequently, the solution of Eq. (33) can be written as

$$\tilde{v} = c_1\sin(\lambda_1\xi) + c_2\cos(\lambda_1\xi) + c_3\sinh(\lambda_2\xi) + c_4\cosh(\lambda_2\xi) + c_5\sinh(\lambda_3\xi) + c_6\cosh(\lambda_3\xi). \tag{38}$$

The constant $c_i (i = 1, 2, \ldots, 6)$ can be determined by the boundary conditions which lead to the frequencies and mode shapes for free vibrations. Substitution of Eq. (38) into the boundary conditions (29)–(31) yields

$$[\mathbf{A}]\{\mathbf{c}\} = \{\mathbf{0}\}, \tag{39}$$

where [**A**] is described in detail in Appendix B for specified boundary conditions and {**c**} is consisted of the six integral constants $c_i (i = 1, 2, \ldots, 6)$ as follows:

$$\{\mathbf{c}\} = \begin{bmatrix} c_1 & c_2 & c_3 & c_4 & c_5 & c_6 \end{bmatrix}^{\mathrm{T}}. \tag{40}$$

A non-trivial solution of the constants $c_i (i = 1, 2, \ldots, 6)$ can be obtained only when the determinant of the coefficient matrix in Eq. (39) vanishes. In this manner, the following frequency equations for four cases are determined:

$$|\mathbf{A}| = 0. \tag{41}$$

In general, the frequency Eq. (41) is transcendental with respect to the frequency $\tilde{\omega}$, so the trial method can be used to find their roots. In detail, the frequency $\tilde{\omega}$ is stepped through a sequence of small increments and the sign of the determinant of the matrix [**A**] is computed for each value of $\tilde{\omega}$ and recorded. After a sufficient number of sign crossings have been identified, the value of $\tilde{\omega}$ that satisfies Eq. (41) can be isolated and refined using bisection.

It should be noted that an exact solution of the frequency can be obtained for an SS member through simplifying the first one of Eq. (41), which is

$$\tilde{\omega}_n^2 = \tilde{\omega}_{n0}^2 \left[1 + \frac{\tilde{H}}{\tilde{N}_{n,\mathrm{cr}}} - \frac{\beta^2 - 1}{\tilde{\alpha}^2/(n\pi)^2 + \beta^2} \right], \tag{42}$$

where $\tilde{\omega}_{n0}$ denotes the nth-order non-dimensional frequency of full-interaction composite beam without axial force and is defined as

$$\tilde{\omega}_{n0}^2 = \frac{mL^4}{\overline{EI}} \omega_{n0}^2 \tag{43}$$

in which ω_{n0} is the nth-order frequency of a full-interaction composite beam with SS ends

$$\omega_{n0}^2 = \left(\frac{n\pi}{L} \right)^4 \frac{\overline{EI}}{m}. \tag{44}$$

And $\tilde{N}_{n,\mathrm{cr}}$ denotes the nth-order critical axial force of a full-interaction composite member with SS ends in dimensionless form

$$\tilde{N}_{n,\mathrm{cr}} = \frac{L^2}{\overline{EI}} N_{n,\mathrm{cr}} \tag{45}$$

in which the symbol $N_{n,\mathrm{cr}}$ signifies the nth-order critical axial force, i.e.,

$$N_{n,\mathrm{cr}} = \left(\frac{n\pi}{L} \right)^2 \overline{EI} \tag{46}$$

of an SS beam.

It is readily found, from Eq. (42), that the axial force and the interlayer slip independently affect the frequencies of the composite beam when its two ends are simply supported. A tensile force enlarges the frequencies while a compressive force reduces the frequencies of a partial-interaction composite member, which is similar to the case of full-interaction composite beams. Since $\beta^2 > 1$ (see its definition in the second one of Eq. (22)) always holds, the last item in the square bracket of Eq. (42), which implies the effect of the stiffness of the shear connectors, leads to the decrease of the frequencies of partial-interaction composite members compared with full-interaction composite ones. If the composite member is bonded perfectly, i.e., no slip occurs at the interface, the parameter $\tilde{\alpha}^2$, which reflects the rigidity of the shear connectors, will approach infinite, Eq. (42) becomes

$$\tilde{\omega}_n^2 = \tilde{\omega}_{n0}^2 \left(1 + \frac{\tilde{H}}{\tilde{N}_{n,\mathrm{cr}}} \right) \tag{47}$$

which has been obtained by Weaver et al. [15].

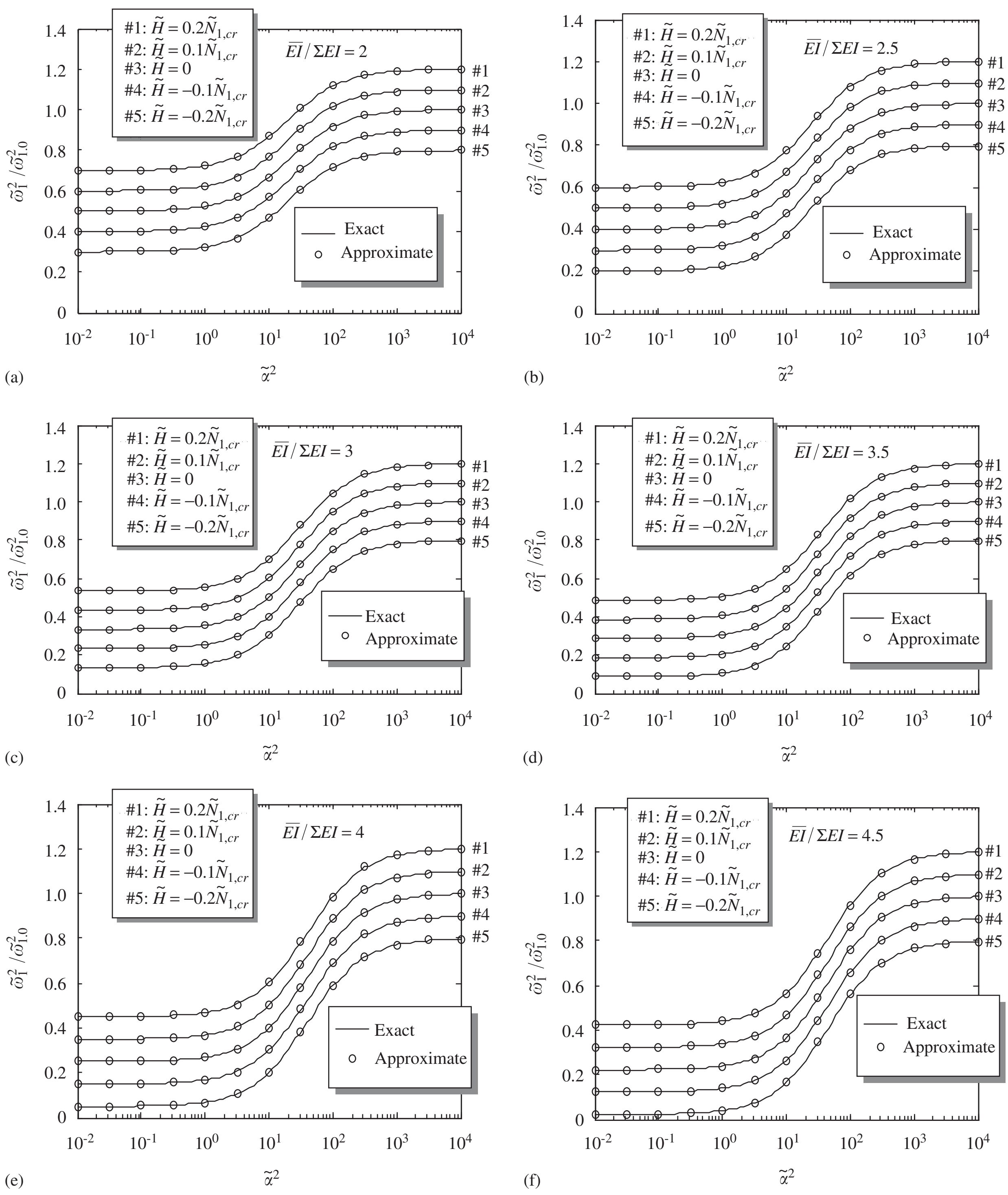

Fig. 5. Relative fundamental frequencies $\tilde{\omega}_1^2/\tilde{\omega}_{1,0}^2$ versus $\tilde{\alpha}^2$ for different values of β^2 under different axial force $\tilde{H}$ for SS cases.

In Eq. (42), the frequency decreases with the axially compressive force. The critical axial load $\tilde{H}_{n,\mathrm{cr}}$ of the buckling of the partial-interaction composite member can be obtained when the frequency approaches zero, namely >

$$\tilde{H}_{n,\mathrm{cr}} = \frac{\tilde{\alpha}^2 + (n\pi)^2}{\tilde{\alpha}^2 + \beta^2 (n\pi)^2}\, \tilde{N}_{n,\mathrm{cr}}. \tag{48}$$

This agrees with the result of Girhammar and Gopu [4].

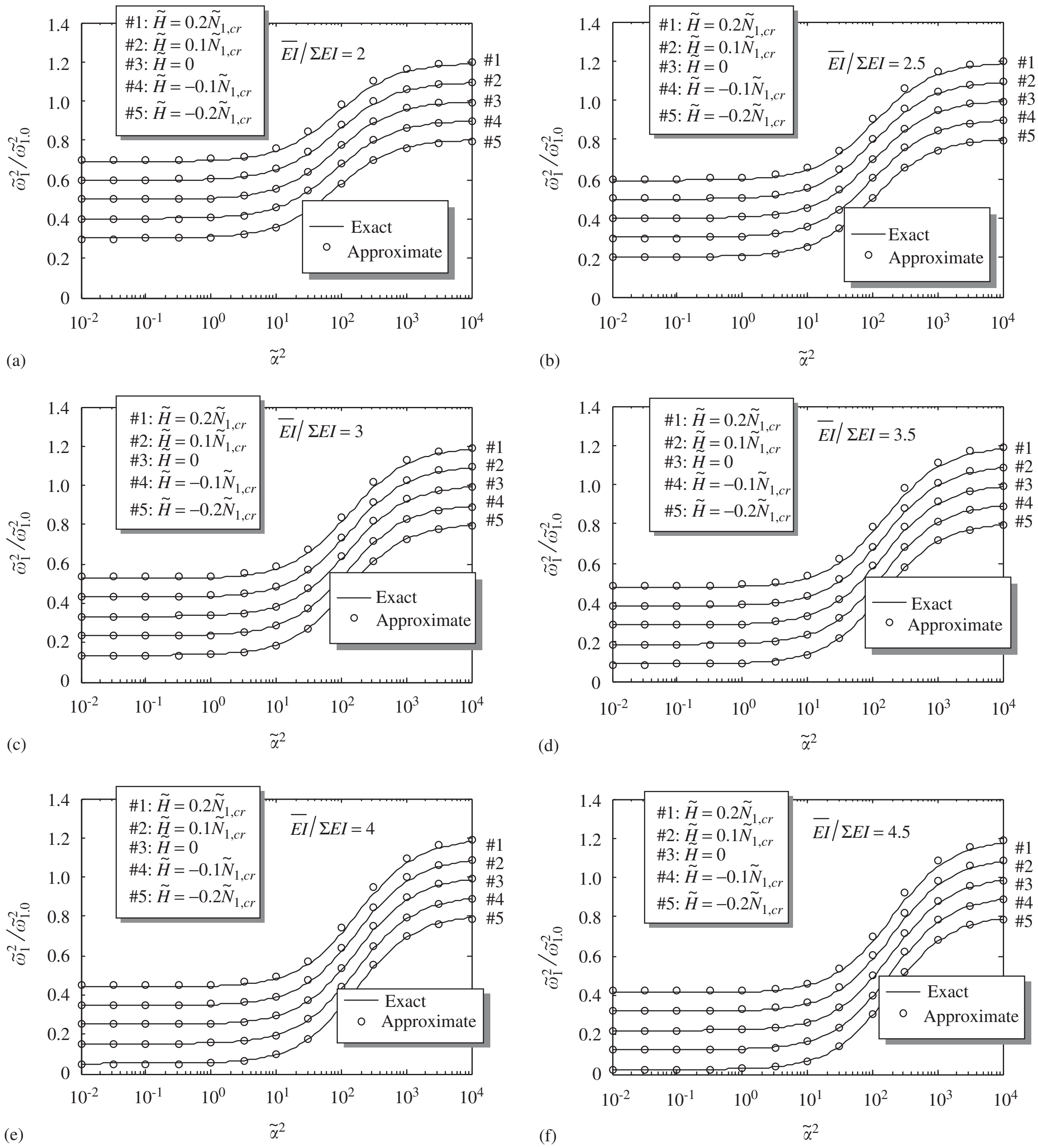

Fig. 6. Relative fundamental frequencies $\tilde{\omega}_1^2/\tilde{\omega}_{1,0}^2$ versus $\tilde{\alpha}^2$ for different values of β^2 under different axial force $\tilde{H}$ for CC cases.

In the general case of arbitrary boundary conditions, the frequencies are obtained from transcendental equation (41), which require numerical solutions described in the preceding section. Usually, the fundamental frequency is of most importance in practice. In consideration of Eq. (42), an approximate expression is proposed as

$$\tilde{\omega}_1^2 = \tilde{\omega}_{1,0}^2\left[1 \pm \left(\frac{|\tilde{H}|}{\tilde{N}_{1,\mathrm{cr}}}\right)^{\gamma} - \frac{\beta^2 - 1}{\tilde{\alpha}^2/(\mu\pi)^2 + \beta^2}\right] \tag{49}$$

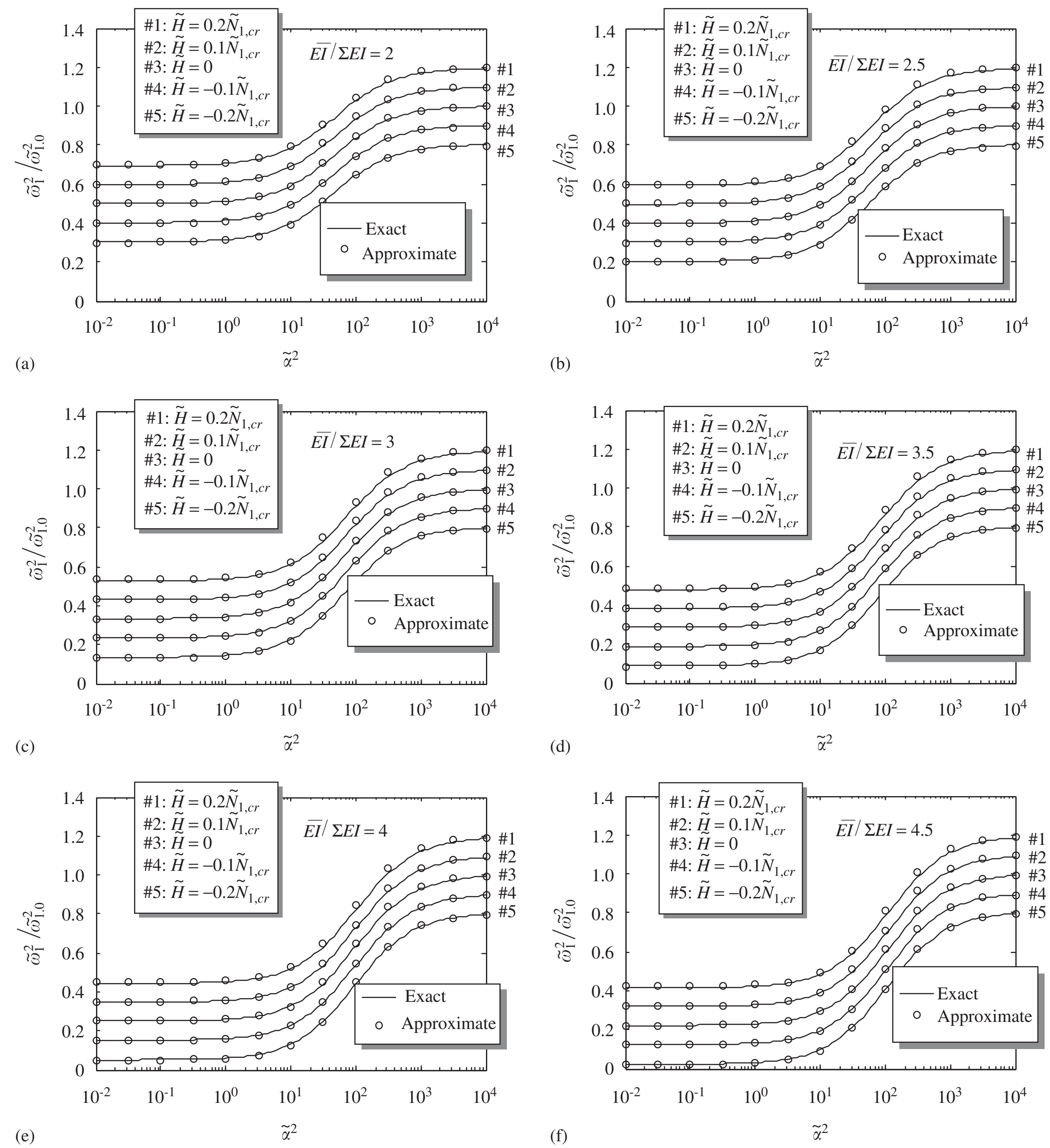

Fig. 7. Relative fundamental frequencies $\tilde{\omega}_1^2/\tilde{\omega}_{1,0}^2$ versus $\tilde{\alpha}^2$ for different values of β^2 under different axial force $\tilde{H}$ for SC cases.

to predict the fundamental frequencies of the partial-interaction composite members in which the plus and minus symbols correspond to tensile and compressive axial forces, respectively. The critical axial load $\tilde{N}_{1,\mathrm{cr}}$ and the parameters μ and γ in Eq. (49) are determined from numerical regression analyses for different boundary

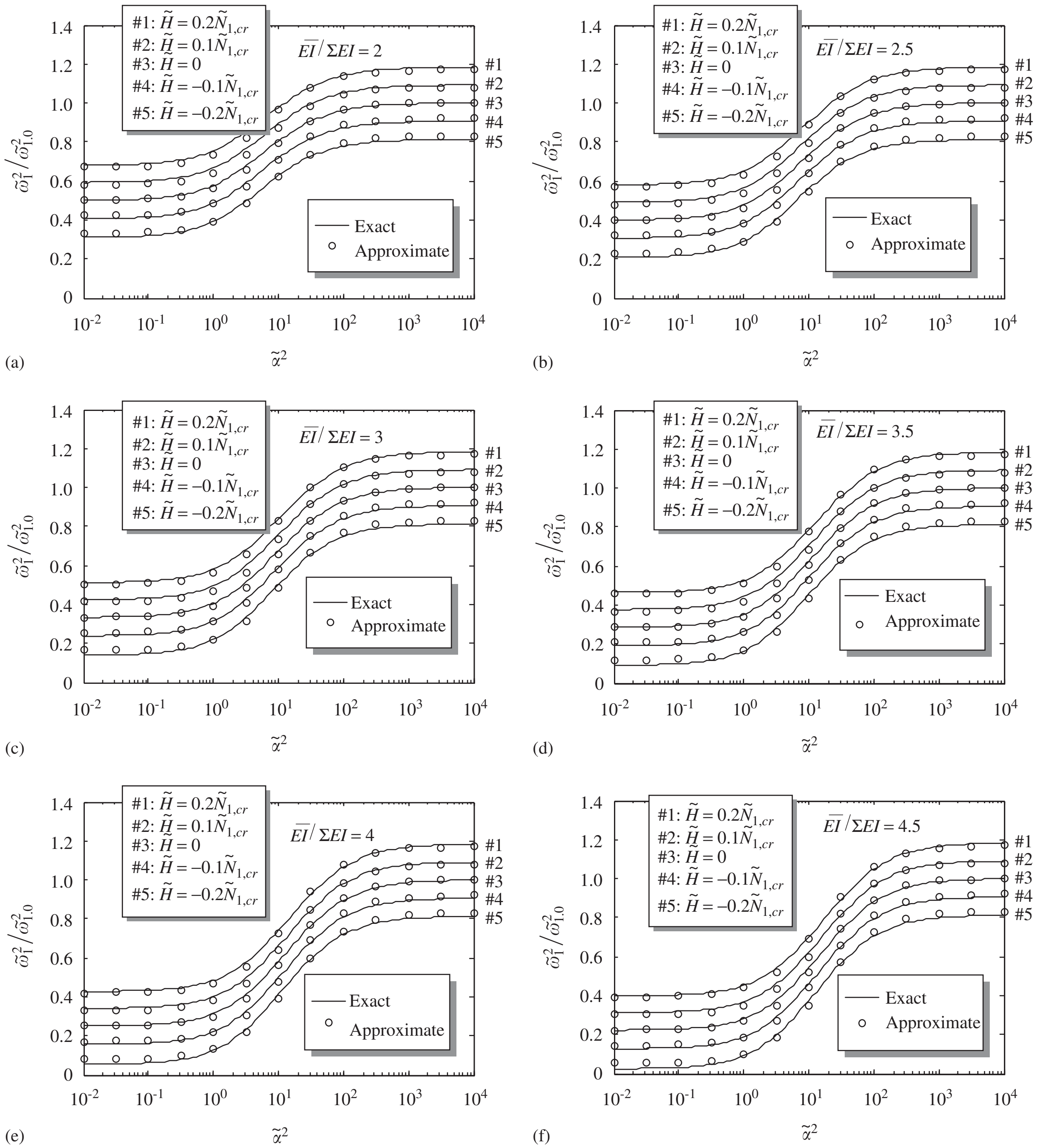

Fig. 8. Relative fundamental frequencies $\tilde{\omega}_1^2/\tilde{\omega}_{1,0}^2$ versus $\tilde{\alpha}^2$ for different values of β^2 under different axial force $\tilde{H}$ for CF cases.

conditions and are calculated to be

$$\begin{aligned} &\tilde{N}_{1,\mathrm{cr}} = \pi^2, && \mu = 1.0, && \gamma = 1.00 && \text{for SS},\\ &\tilde{N}_{1,\mathrm{cr}} = 4\pi^2, && \mu = 2.0, && \gamma = 1.03 && \text{for CC},\\ &\tilde{N}_{1,\mathrm{cr}} = 0.25\pi^2, && \mu = 0.5, && \gamma = 1.10 && \text{for CF},\\ &\tilde{N}_{1,\mathrm{cr}} = 2.045\pi^2, && \mu = 1.5, && \gamma = 1.03 && \text{for SC}. \end{aligned} \tag{50}$$

In fact, the critical axial loads $\tilde{N}_{1,\mathrm{cr}}$ for four boundary conditions coincide with those from the elementary beam theory.

4. Numerical examples and discussions

In this section, numerical examples are presented for illustrating the proposed method and depicting the effect of the axial load and the shear rigidity of the shear connector upon the frequencies of the partial-interaction composite members. Figs. 5–8 show that the relative frequency $\tilde{\omega}_1^2/\tilde{\omega}_{1,0}^2$ varies in a similar way with respect to the parameter $\tilde{\alpha}^2$ for four end conditions. It is the parameter $\tilde{\alpha}^2$ that has a sensitive range, in which the relative frequency is affected more significantly by $\tilde{\alpha}^2$. If $\tilde{\alpha}^2$ does not locate in this range, variation of the value of $\tilde{\omega}_1^2/\tilde{\omega}_{1,0}^2$ is insignificant. The ranges are different for four boundary conditions, which are $\tilde{\alpha}^2 \in [10^0, 10^{2.5}]$ for SS, $\tilde{\alpha}^2 \in [10^1, 10^4]$ for CC, $\tilde{\alpha}^2 \in [10^{0.5}, 10^3]$ for SC and $\tilde{\alpha}^2 \in [10^{-0.5}, 10^{2.5}]$ for CF. In fact, it can be found that the frequencies are almost independent of $\tilde{\alpha}^2$ when $\tilde{\alpha}^2/(\mu\pi)^2 \ll \beta^2$ or $\tilde{\alpha}^2/(\mu\pi)^2 \gg \beta^2$, since the last term in the square bracket of Eq. (49) is independent of $\tilde{\alpha}^2$ or vanishes in the two cases, respectively.

Figs. 9–12 demonstrate the effect of the parameter $\beta^2 = \overline{EI}/\Sigma EI$ upon the relative frequency $\tilde{\omega}_1^2/\tilde{\omega}_{1,0}^2$ under four end conditions. It is readily found that their relation approaches linearity gradually from a sagging curve with the increase of the parameter $\tilde{\alpha}^2$. Simultaneously, the approached lines also become horizontal with the increase of the parameter $\tilde{\alpha}^2$, which implies that the relative frequency $\tilde{\omega}_1^2/\tilde{\omega}_{1,0}^2$ is insignificantly affected by the parameter β^2 for composite members with large $\tilde{\alpha}^2$ value. This can be clearly seen from Eq. (49) for $\tilde{\alpha}^2/(\mu\pi)^2 \gg \beta^2$. When β^2 approaches 1 ($\beta^2 = \overline{EI}/\Sigma EI > 1$), all the curves in Figs. 9–12 approache the value of 0.9, which can also be found from Eq. (49).

The effects of the axial force upon the frequency are illustrated in Figs. 13–16 for four end conditions. A perfectly linear relation between the axial force $\tilde{H}/\tilde{N}_{1,\mathrm{cr}}$ and the relative frequency $\tilde{\omega}_1^2/\tilde{\omega}_{1,0}^2$ is shown both in

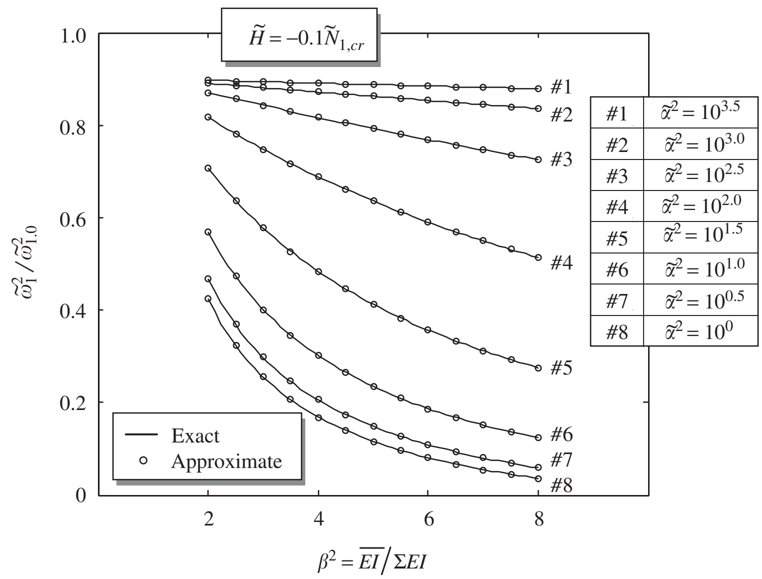

Fig. 9. Relative frequency parameter $\tilde{\omega}_1^2/\tilde{\omega}_{1,0}^2$ versus parameter β^2 for SS cases.

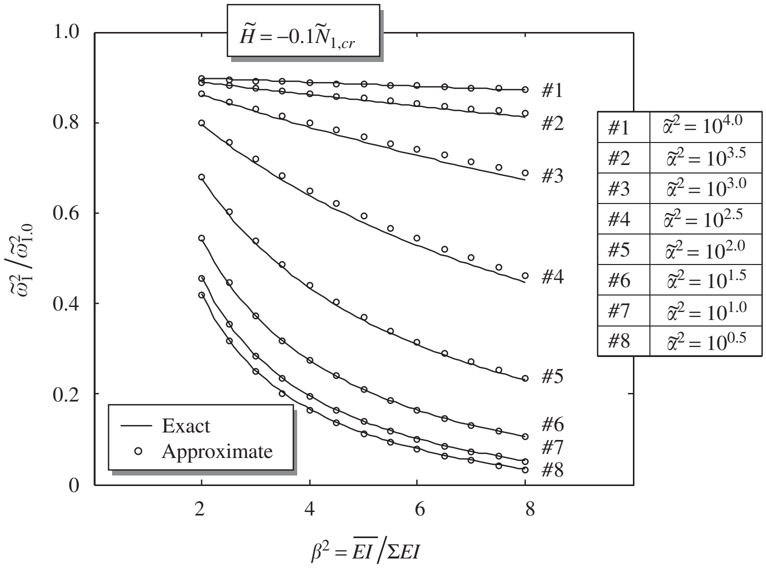

Fig. 10. Relative frequency parameter $\tilde{\omega}_1^2/\tilde{\omega}_{1,0}^2$ versus parameter β^2 for CC cases.

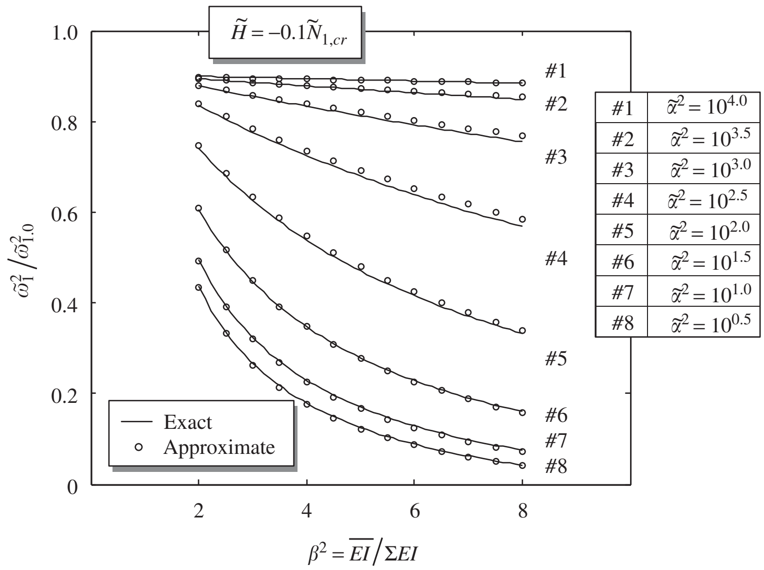

Fig. 11. Relative frequency parameter $\tilde{\omega}_1^2/\tilde{\omega}_{1,0}^2$ versus parameter β^2 for SC cases.

Eq. (49) and Fig. 13 for SS cases. However, their relation is slightly non-linear for other three end conditions as shown in Figs. 14–16. Thus an exponent γ, whose value is near 1 and given in Eq. (50), is introduced in the approximate expression (49). Figs. 13–16 also show the fact that the influence of the axial force is independent of the parameter $\tilde{\alpha}^2$ for all four boundary conditions, since the solid lines corresponding to the exact solutions have the same form with different parameter $\tilde{\alpha}^2$. These phenomena are also displayed in Figs. 9–12. It implies that the effects of axial force on the fundamental frequency of partial-interaction composite members are independent of the degree of the shear connection of the composite members. In other words, the influence of the axial force on the frequency is the same for both a non-interaction member ($k_s = 0$) and a full-interaction member ($k_s \to \infty$).

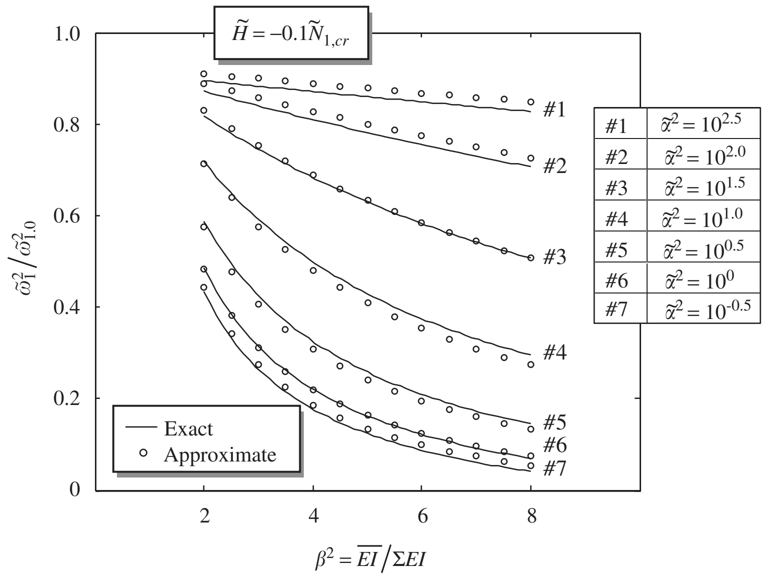

Fig. 12. Relative frequency parameter $\tilde{\omega}_1^2/\tilde{\omega}_{1,0}^2$ versus parameter β^2 for CF cases.

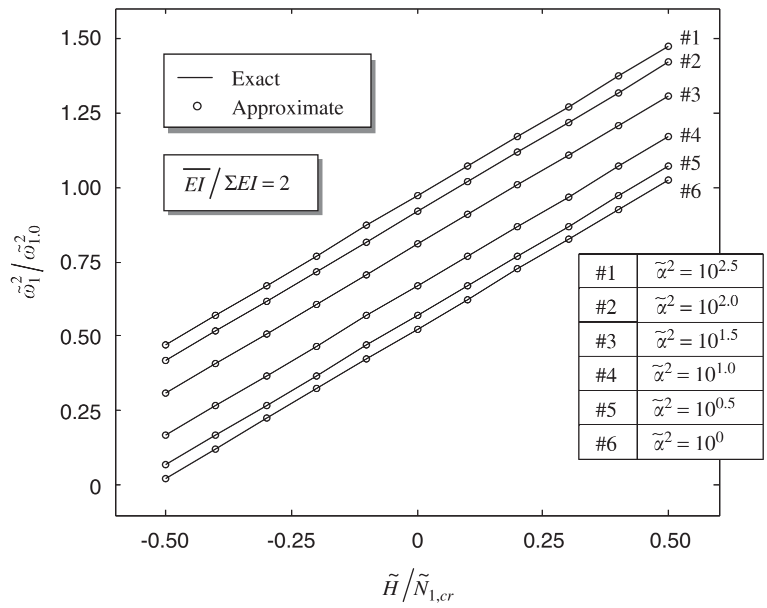

Fig. 13. Relative frequency parameter $\tilde{\omega}_1^2/\tilde{\omega}_{1,0}^2$ versus axial force $\tilde{H}/\tilde{N}_{1,cr}$ for SS cases.

5. Conclusions

1. The governing differential equations of motion are derived for the partial-interaction composite members with axial force and the solutions of free vibrations are presented under common boundary conditions. If the slip at the interface of the composite members is ignored, the equations can be degenerated to those from the elementary beam theory, as expected.
2. An exact solution for the simply supported cases is obtained while approximate and simple ones for other boundary conditions are proposed to predict the fundamental frequency of the partial-interaction

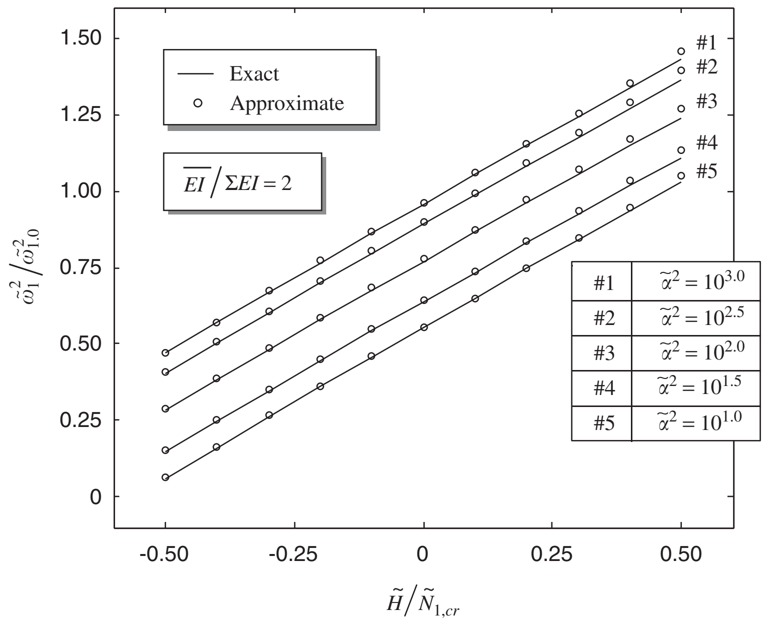

Fig. 14. Relative frequency parameter $\tilde{\omega}_1^2/\tilde{\omega}_{1,0}^2$ versus axial force $\tilde{H}/\tilde{N}_{1,\mathrm{cr}}$ for CC cases.

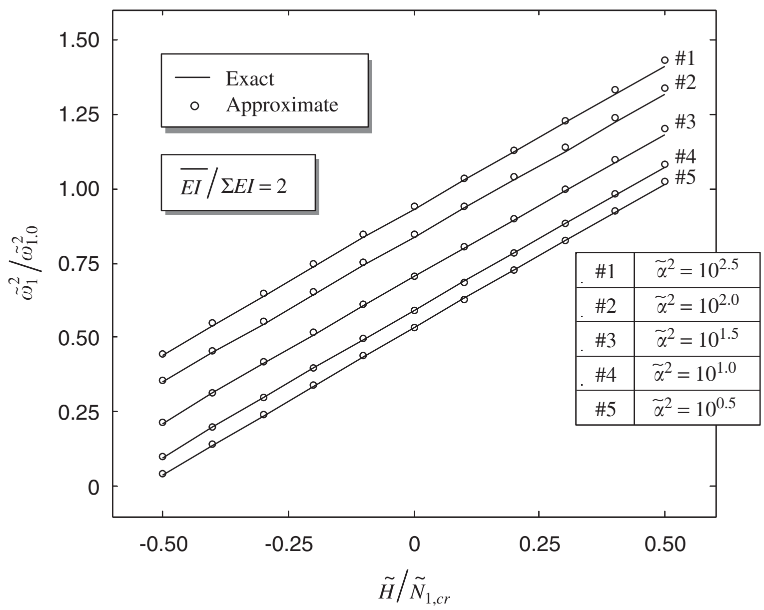

Fig. 15. Relative frequency parameter $\tilde{\omega}_1^2/\tilde{\omega}_{1,0}^2$ versus axial force $\tilde{H}/\tilde{N}_{1,\mathrm{cr}}$ for SC cases.

composite members with axial force. The exact solution can also be degenerated to that for the case of a full-interaction composite member, which has been available in literatures.

3. The results show the fact that the effects of the axial force upon the frequencies are independent of the degree of the shear connection of partial-interaction composite members.
4. The parameter $\tilde{\alpha}^2$ has a sensitive range, in which the frequency is affected significantly by $\tilde{\alpha}^2$, and outside which its effect is insignificant. The influence of the parameter β^2 is coupled with the parameter $\tilde{\alpha}^2$.

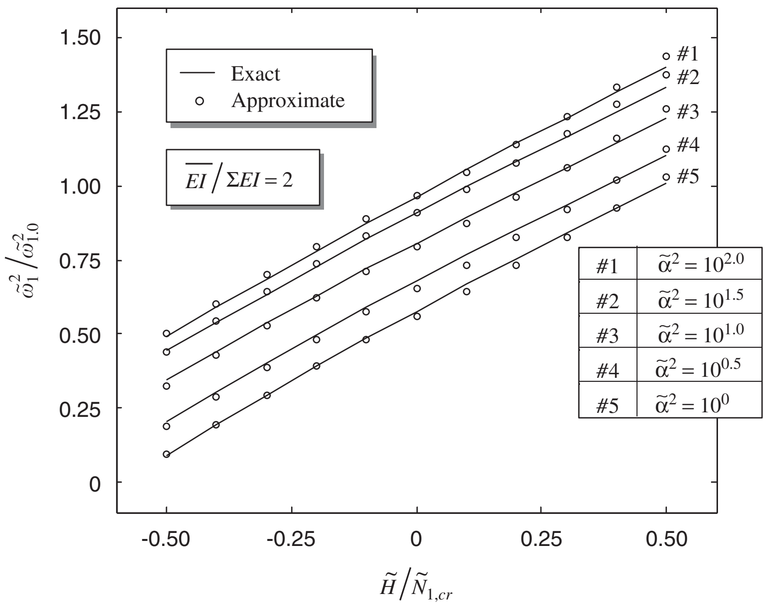

Fig. 16. Relative frequency parameter $\tilde{\omega}_1^2/\tilde{\omega}_{1,0}^2$ versus axial force $\tilde{H}/\tilde{N}_{1,\mathrm{cr}}$ for CF cases.

The relation of β^2 with the relative frequency approaches a horizontal line from a sagging curve with the increase of the parameter $\tilde{\alpha}^2$.

Acknowledgement

The work described in this paper was fully supported by a grant from the Research Grant Council of the Hong Kong Special Administrative Region, China [Project no. CityU 1113/04E].

Appendix A

In this section, it will be shown that Eq. (36) has three real roots, with one being negative and the other two positive. The standard form of a cubic equation in one variable can be written as

$$x^3 + ax^2 + bx + c = 0, \tag{A.1}$$

where a, b and c are real. Its discriminant D is given by [16]

$$D = \frac{p^3}{27} + \frac{q^2}{4} \tag{A.2}$$

in which

$$p = -\frac{a^2}{3} + b, \quad q = \frac{2a^3}{27} - \frac{ab}{3} + c. \tag{A.3}$$

If the discriminant is negative, i.e., $D<0$, Eq. (A.1) has three real roots x_1, x_2 and x_3, and they satisfy

$$x_1 + x_2 + x_3 = -a, \quad x_1x_2 + x_2x_3 + x_3x_1 = b, \quad x_1x_2x_3 = -c. \tag{A.4}$$

According to Eq. (36), the coefficients a, b and c of the cubic equation (A.1) are

$$a = -(\tilde{\alpha}^2 + \beta^2 \tilde{H}), \quad b = -(\beta^2 \tilde{\omega}_n^2 - \tilde{\alpha}^2 \tilde{H}), \quad c = \tilde{\alpha}^2 \tilde{\omega}_n^2. \tag{A.5}$$

Consequently, the discriminant of Eq. (36) can be calculated. To avoid the calculation of fraction number, another constant R is introduced as

$$R = -108D. \tag{A.6}$$

By introducing $t = 1/\beta^2$, through some algebraic operations, we get

$$R = A^2 + B + 4\tilde{\omega}^2(C^2 + E^2 + F\tilde{\omega}^4\beta^6), \tag{A.7}$$

where

$$A = \tilde{\alpha}^2\beta^2\tilde{H}^2 + \tilde{\omega}^2\beta^4\tilde{H} - (2t-1)\tilde{\alpha}^4\tilde{H} + \tilde{\omega}^2\tilde{\alpha}^2\beta^2 - \tilde{\omega}^2\tilde{\alpha}^2, \tag{A.8}$$

$$B = 4t(1-t)\tilde{\alpha}^8\tilde{H}^2, \tag{A.9}$$

$$C = \tilde{\alpha}^2\beta^2\tilde{H}^2 - \tfrac{1}{2}(t^2 + 3t - 2)\tilde{\alpha}^4 + \tilde{\omega}^2\beta^2, \tag{A.10}$$

$$E = \sqrt{1 - (t^2 + 3t - 2)^2/4}\,\tilde{\alpha}^4 + \frac{t + 3\beta^2 - 4}{2\sqrt{1 - (t^2 + 3t - 2)^2/4}}\,\tilde{\omega}^2 \tag{A.11}$$

and

$$F = \frac{(1-t)(13t+3)}{(t+3)(t+4)}. \tag{A.12}$$

Since $\beta^2 > 1$, i.e., $0 < t < 1$, it can be concluded that $1 - (t^2 + 3t - 2)^2/4 > 0$ in the expression of E in Eq. (A.11) and $B > 0$, $F > 0$. Thus, R in Eq. (A.7) is always positive, namely, the discriminant D in Eq. (A.2) is negative and Eq. (36) has three real roots.

From the last of Eq. (A.4), all or only one of the three real roots should be negative because of $x_1x_2x_3 = -c = -\tilde{\alpha}^2\tilde{\omega}^2 < 0$. If all the three real roots are negative, both the coefficients a and b should be positive since the first two of Eq. (A.4) hold. However, at least one of the coefficients a and b is negative because it can be readily shown that $a < 0$ for $\tilde{H} \geq 0$ and $b < 0$ for $\tilde{H} \leqslant 0$ by using their definition in the first two of Eq. (A.5). As a result, one of the three real roots of Eq. (36) is negative and the other two are positive.

Appendix B

For SS, SC, CC and CF beams, the coefficient matrix [**A**] is given by

$$[\mathbf{A}] = \begin{bmatrix} \mathbf{A}_S(0) \\ \mathbf{A}_S(1) \end{bmatrix}, \quad [\mathbf{A}] = \begin{bmatrix} \mathbf{A}_S(0) \\ \mathbf{A}_C(1) \end{bmatrix}, \quad [\mathbf{A}] = \begin{bmatrix} \mathbf{A}_C(0) \\ \mathbf{A}_C(1) \end{bmatrix}, \quad [\mathbf{A}] = \begin{bmatrix} \mathbf{A}_C(0) \\ \mathbf{A}_F(1) \end{bmatrix}, \tag{B.1}$$

respectively, where the coefficient matrix $[\mathbf{A}_S(0)]$ denotes the value of $[\mathbf{A}_S]$ at $\xi = 0$ and so on. The matrices $[\mathbf{A}_S]$, $[\mathbf{A}_C]$ and $[\mathbf{A}_F]$ can also be written as

$$[\mathbf{A}_S] = [\,\mathbf{A}_{S1} \quad \mathbf{A}_{S2} \quad \mathbf{A}_{S3}\,], \tag{B.2}$$

$$[\mathbf{A}_C] = [\,\mathbf{A}_{C1} \quad \mathbf{A}_{C2} \quad \mathbf{A}_{C3}\,], \tag{B.3}$$

$$[\mathbf{A}_F] = [\,\mathbf{A}_{F1} \quad \mathbf{A}_{F2} \quad \mathbf{A}_{F3}\,], \tag{B.4}$$

where

$$[\mathbf{A}_{S1}] = \begin{bmatrix} \sin(\lambda_1\xi) & \cos(\lambda_1\xi) \\ -\lambda_1^2 \sin(\lambda_1\xi) & -\lambda_1^2 \cos(\lambda_1\xi) \\ \lambda_1^4 \sin(\lambda_1\xi) & \lambda_1^4 \cos(\lambda_1\xi) \end{bmatrix}, \tag{B.5}$$

$$[\mathbf{A}_{S2}] = \begin{bmatrix} \sinh(\lambda_2\xi) & \cosh(\lambda_2\xi) \\ \lambda_2^2 \sinh(\lambda_2\xi) & \lambda_2^2 \cosh(\lambda_2\xi) \\ \lambda_2^4 \sinh(\lambda_2\xi) & \lambda_2^4 \cosh(\lambda_2\xi) \end{bmatrix}, \tag{B.6}$$

$$[\mathbf{A}_{S3}] = \begin{bmatrix} \sinh(\lambda_3\xi) & \cosh(\lambda_3\xi) \\ \lambda_3^2 \sinh(\lambda_3\xi) & \lambda_3^2 \cosh(\lambda_3\xi) \\ \lambda_3^4 \sinh(\lambda_3\xi) & \lambda_3^4 \cosh(\lambda_3\xi) \end{bmatrix}, \tag{B.7}$$

$$[\mathbf{A}_{C1}] = \begin{bmatrix} \sin(\lambda_1\xi) & \cos(\lambda_1\xi) \\ \lambda_1 \cos(\lambda_1\xi) & -\lambda_1 \sin(\lambda_1\xi) \\ (\lambda_1^5 + \gamma_1\lambda_1^3)\cos(\lambda_1\xi) & -(\lambda_1^5 + \gamma_1\lambda_1^3)\sin(\lambda_1\xi) \end{bmatrix}, \tag{B.8}$$

$$[\mathbf{A}_{C2}] = \begin{bmatrix} \sinh(\lambda_2\xi) & \cosh(\lambda_2\xi) \\ \lambda_2 \cosh(\lambda_2\xi) & \lambda_2 \sinh(\lambda_2\xi) \\ (\lambda_2^5 - \gamma_1\lambda_2^3)\cosh(\lambda_2\xi) & (\lambda_2^5 - \gamma_1\lambda_2^3)\sinh(\lambda_2\xi) \end{bmatrix}, \tag{B.9}$$

$$[\mathbf{A}_{C3}] = \begin{bmatrix} \sinh(\lambda_3\xi) & \cosh(\lambda_3\xi) \\ \lambda_3 \cosh(\lambda_3\xi) & \lambda_3 \sinh(\lambda_3\xi) \\ (\lambda_3^5 - \gamma_1\lambda_3^3)\cosh(\lambda_3\xi) & (\lambda_3^5 - \gamma_1\lambda_3^3)\sinh(\lambda_3\xi) \end{bmatrix}, \tag{B.10}$$

$$[\mathbf{A}_{F1}] = \begin{bmatrix} -\lambda_1^2 \sin(\lambda_1\xi) & -\lambda_1^2 \cos(\lambda_1\xi) \\ (\lambda_1^4 - \gamma_2)\sin(\lambda_1\xi) & (\lambda_1^4 - \gamma_2)\cos(\lambda_1\xi) \\ (\lambda_1^5 + \gamma_3\lambda_1^3 - \gamma_4\lambda_1)\cos(\lambda_1\xi) & -(\lambda_1^5 + \gamma_3\lambda_1^3 - \gamma_4\lambda_1)\sin(\lambda_1\xi) \end{bmatrix}, \tag{B.11}$$

$$[\mathbf{A}_{F2}] = \begin{bmatrix} \lambda_2^2 \sinh(\lambda_2\xi) & \lambda_2^2 \cosh(\lambda_2\xi) \\ (\lambda_2^4 - \gamma_2)\sinh(\lambda_2\xi) & (\lambda_2^4 - \gamma_2)\cosh(\lambda_2\xi) \\ (\lambda_2^5 - \gamma_3\lambda_2^3 - \gamma_4\lambda_2)\cosh(\lambda_2\xi) & (\lambda_2^5 - \gamma_3\lambda_2^3 - \gamma_4\lambda_2)\sinh(\lambda_2\xi) \end{bmatrix}, \tag{B.12}$$

$$[\mathbf{A}_{F3}] = \begin{bmatrix} \lambda_3^2 \sinh(\lambda_3\xi) & \lambda_3^2 \cosh(\lambda_3\xi) \\ (\lambda_3^4 - \gamma_2)\sinh(\lambda_3\xi) & (\lambda_3^4 - \gamma_2)\cosh(\lambda_3\xi) \\ (\lambda_3^5 - \gamma_3\lambda_3^3 - \gamma_4\lambda_3)\cosh(\lambda_3\xi) & (\lambda_3^5 - \gamma_3\lambda_3^3 - \gamma_4\lambda_3)\sinh(\lambda_3\xi) \end{bmatrix} \tag{B.13}$$

and the parameters γ_1, γ_2, γ_3 and γ_4 are defined as

$$\gamma_1 = \tilde{\alpha}^2 - \tilde{\alpha}^2/\beta^2 + \beta^2\tilde{H}, \quad \gamma_2 = \beta^2\tilde{\omega}^2, \quad \gamma_3 = \tilde{\alpha}^2 + \beta^2\tilde{H}, \quad \gamma_4 = \beta^2\tilde{\omega}^2 - \tilde{\alpha}^2\tilde{H}. \tag{B.14}$$

References

[1] Y.F. Wu, M.C. Griffith, D.J. Oehlers, Improving the strength and ductility of rectangular RC columns through composite partial-interaction: tests, *Journal of Structural Engineering, ASCE* 129 (9) (2003) 1183–1190.

[2] N.M. Newmark, C.P. Siess, I.M. Viest, Test and analysis of composite beams with incomplete interaction, *Proceedings of the Society for Experimental Stress and Analysis* 9 (1) (1951) 75–92.

[3] Goodman JR. Layered wood systems with interlayer slip, PhD Thesis, University of California, Berkeley, California, 1967.
[4] U.A. Girhammar, V.K.A. Gopu, Composite beam-columns with interlayer slip-exact analysis, *Journal of Structural Engineering, ASCE* 119 (4) (1993) 1265–1282.
[5] Y.C. Wang, Deflection of steel-concrete composite beams with partial shear interaction, *Journal of Structural Engineering, ASCE* 124 (10) (1998) 1159–1165.
[6] Y.F. Wu, D.J. Oehlers, M.C. Griffith, Partial-interaction analysis of composite beam/column members, *Mechanics of Structures and Machines* 30 (3) (2002) 309–332.
[7] G. Fabbrocino, G. Manfredi, E. Cosenza, Analysis of continuous composite beams including partial interaction and bond, *Journal of Structural Engineering, ASCE* 126 (11) (2000) 1288–1294.
[8] R. Seracino, C.T. Lee, T.C. Lim, J.Y. Lim, Partial interaction stresses in continuous composite beams under serviceability loads, *Journal of Constructional Steel Research* 60 (10) (2004) 1525–1543.
[9] L.X. Fang, S.L. Chan, Y.L. Wong, Numerical analysis of composite frames with partial shear-stud interaction by one element per member, *Engineering Structures* 22 (10) (2000) 1285–1300.
[10] M.R. Salari, E. Spacone, Finite element formulations of one-dimensional elements with bond-slip, *Engineering Structures* 23 (7) (2001) 815–826.
[11] G. Ranzi, M.A. Bradford, B. Uy, A direct stiffness analysis of a composite beam with partial interaction, *International Journal for Numerical Methods in Engineering* 61 (5) (2004) 657–672.
[12] Y.F. Wu, M.C. Griffith, D.J. Oehlers, Numerical simulation of steel plated RC column, *Computers and Structures* 82 (4–5) (2004) 359–371.
[13] U.A. Girhammar, D. Pan, Dynamic analysis of composite members with interlayer slip, *International Journal of Solids and Structures* 30 (6) (1993) 797–823.
[14] C. Adam, A. Jeschko, Flexural vibrations of elastic composite beams with interlayer slip, *Acta Mechanica* 125 (1–4) (1997) 17–30.
[15] W. Weaver, S.P. Timoshenko, D.H. Young, *Vibration Problems in Engineering*, Wiley, New York, 1990.
[16] H.J. Bartsch, *Handbook of Mathematical Formulas*, Academic Press, Inc., New York, 1974.